J. Phys. B: At. Mol. Opt. Phys. 25 (1992) 3175–3185. Printed in the UK

# Electron impact ionization of Cr ($3d^5 4s$) $^7S$

R H G Reid†, K Bartschat‡ and P G Burke†

† School of Mathematics and Physics, The Queen's University of Belfast, Belfast BT7 1NN, UK

‡ Department of Physics and Astronomy, Drake University, Des Moines, IA 50311, USA

Received 5 May 1992

**Abstract.** The $R$-matrix method of Bartschat and Burke (1987) has been used to calculate total and single differential cross sections for electron impact ionization of Cr I in its ground $^7S$ state for impact energies from near threshold to 100 eV. The total cross section for ionization has a peak value of $30.3\,a_0^2$ at an impact energy of 31 eV. For energies above 30 eV, the total cross section for the production of $Cr^+$ ($3d^4 4s$) $^6D$ is significantly greater than that for production of $Cr^+$ ($3d^5$) $^6S$, while for energies below 30 eV the reverse is true. The single differential cross section exhibits pronounced resonance structure for energy losses of the incident electron that are below the threshold for $Cr^+$ ($3d^4 4s$) $^6D$ production. These resonances have been analysed in detail.

## 1. Introduction

We have calculated total and single differential cross sections for electron impact ionization of Cr ($3d^5 4s$) $^7S$ using the $R$-matrix method of Bartschat and Burke (1987). This is a 'DCBNX' method (cf Jacubowicz and Moores 1981), in that the ionizing electron is described by distorted waves, and no account is taken of exchange between the ionizing and the ejected electron, except for taking the upper limit of the ejected-electron energy to be half the maximum possible value when integrating the single differential cross section. The main merit of this method lies in its accurate treatment of the initial bound state and the final continuum states of the target within an inner region in the space of the ejected electron. In this region, which is sufficiently large to contain the initial bound state, exchange and correlation effects are accurately described and a basis of configuration interaction wavefunctions is constructed. These basis functions are independent of the energy of the physical states, whose wavefunctions in the inner region are determined by being joined, at the boundary, to solutions with the correct asymptotic form via the $R$-matrix. Energy dependence arises only in the solution of the coupled equations in the outer region and in the joining procedure, and the former is simplified by the omission of exchange. Hence the $R$-matrix method is much more efficient than a close-coupling method that requires a solution of coupled integro-differential equations at each energy (Jacubowicz and Moores 1981). The accurate representation of the continuum states in the inner region incorporates effects such as autoionization. The consistency in the treatments of the bound state and the continuum states within the inner region is also a notable feature of the $R$-matrix method.

0953-4075/92/143175+11$04.50  

Our interest in Cr as a target arises not only from the fact that it is a complicated system which can demonstrate the merits of the $R$-matrix method, but also because of the need for ionization data for the JET tokamak, where Cr is released from antennae under ICRF heating (Bures *et al* 1990).

In a previous paper (Bartschat *et al* 1990), we presented results for the ionization of Cr at a single impact energy (100 eV), obtained using only up to the quadrupole component of the interaction. In the present paper, we have completed the calculation by extending the impact-energy range and by retaining up to the $2^4$-pole of the interaction. The previous paper describes the main features of the adaptation to Cr of the general theory (Bartschat and Burke 1987), and so in the next section we describe our calculation only in the detail necessary for discussion of the results. The computer codes are described by Bartschat (1992).

## 2. Outline of calculation

We have considered the ionization of $Cr\,(3d^5 4s)\,^7S$ with production of $Cr^+\,(3d^5)\,^6S$ or $Cr^+\,(3d^4 4s)\,^6D$, these being the only possibilities accessible in the independent particle model without breaking the initial $Cr^{2+}\,(3d^4)\,^5D$ core:

$$e_f(E_0, l_0) + Cr\,(3d^5 4s)\,^7S \xrightarrow{E\lambda} e_f(E_1, l_1) + Cr\,(\mathcal{E}\,^7L^\pi) \tag{1a}$$

$$Cr\,(\mathcal{E}\,^7L^\pi) \sim \begin{cases} Cr^+\,(3d^5)\,^6S + e_s(E_2(^6S), l_2) \\ Cr^+\,(3d^4 4s)\,^6D + e_s(E_2(^6D), l_2). \end{cases} \tag{1b}$$

Equation (1$a$) shows the excitation of Cr to a continuum state of symmetry $^7L^\pi$, caused by the $2^\lambda$-pole component of the interaction with the ionizing electron, $e_f$, which has incident energy $E_0$ and suffers an energy loss $\Delta E \equiv E_0 - E_1$. The effect of the interaction on the Cr system is described by the action of one-electron operators $R^\lambda_{l_0 l_1}(E_0, \Delta E; r_i)$, $r_i$ being the radial coordinate of the $i$th electron in Cr. These are overlaps between incident and outgoing radial waves of $e_f$, with angular momenta $l_0$ and $l_1$, respectively. With an initial S state, the final-state symmetry is uniquely identified by $\lambda$, namely $L = \lambda$ and $\pi = (-1)^\lambda$. We have included all $\lambda \leqslant 4$, and so five continuum states are accessible, with symmetries $^7S^e$, $^7P^o$, $^7D^e$, $^7F^o$ and $^7G^e$.

Equation (1$b$) shows that, in the outer region, the continuum states are comprised of a $Cr^+$ ion and an ejected electron, $e_s$, with energy $E_2(^6S) = \Delta E - I(^6S)$ or $E_2(^6D) = \Delta E - I(^6D)$, where $I(^6S)$ and $I(^6D)$ are the ionization potentials for producing $Cr^+\,(3d^5)\,^6S$ and $Cr^+\,(3d^4 4s)\,^6D$, respectively. We have imposed the empirical values $I(^6S) = 0.497\,2342$ Ryd and $I(^6D) = 0.609\,1208$ Ryd (Bashkin and Stoner 1981). In the outer region, up to the $2^4$-pole components of the $Cr^+ + e_s$ interaction were retained, and partial waves of $e_s$ with angular momentum $l_2 \leqslant 6$ occur.

The $Cr^+\,(3d^5)\,^6S$ and $Cr^+\,(3d^4 4s)\,^6D$ states were represented by single configuration wavefunctions made from the $Cr^+\,(3d^4 4s)\,^6D$ orbitals of Clementi and Roetti (1974), with the 3d and 4s orbitals re-optimized (Bartschat *et al* 1990). To construct Cr states with symmetry up to $^7G^e$, continuum orbitals with angular momentum $l_c \leqslant 6$ were required, and fifteen orbitals ($n_c = 1, \ldots, 15$) were used for each $l_c$. This number is adequate, even for large $E_0$, because the single differential cross sections are peaked at small values of $E_2$. The Cr wavefunctions in the

inner region were thus admixtures of configurations of the form $3d^5(^6S)\,n_c l_c$ or $3d^44s(^6D)\,n_c l_c$, with the all-bound configuration $3d^54s$ also present in the $^7S^e$ states. The numbers of configurations present in the $^7S^e$, $^7P^o$, $^7D^e$, $^7F^o$ and $^7G^e$ states were thus 31, 45, 60, 60 and 60, respectively. Because the empirical ionization potentials were used when calculating the $R$-matrix basis for the continuum states but not the bound state, the $^7S^e$ bound state is not orthogonal to the $^7S^e$ continuum state. Hence it was necessary to include a nuclear term in the interaction when calculating $R^0_{l_0 l_1}(E_0, \Delta E; r_i)$, by taking the monopole component of the interaction to be $1/\max(r_i, r_f) - 1/r_f$, where $r_f$ is the radial coordinate of $e_f$.

In the calculation of $R^\lambda_{l_0 l_1}(E_0, \Delta E; r_i)$, the incident and outgoing partial waves of the ionizing electron were calculated in the static field of Cr ($3d^54s$) $^7S$ as derived from the orbitals of Clementi and Roetti (1974). All $l_0$ and $l_1$ up to $\bar{l}$, say, were retained in the calculation. When $E_0$ is large, the large radius of the 4s orbital makes it necessary to use a large value for $\bar{l}$, and in our previous calculation (Bartschat *et al* 1990) we used $\bar{l} = 50$. To use $\bar{l} = 50$ for $\lambda = 0, \ldots, 4$ would require 732 radial operators for each $E_0$ and $\Delta E$. However, we found that it sufficed to use $\bar{l} = 50$ for $\lambda \leqslant 2$, while using $\bar{l} = 25$ for $\lambda = 3$ or 4. This procedure was necessary only for $E_0 \geqslant 60$ eV. Below 60 eV, we obtained converged results with $\bar{l} = 25$ for all final symmetries.

For each $E_0$, the operators $R^\lambda_{l_0 l_1}(E_0, \Delta E; r)$ were calculated only at five 'key' values of $\Delta E$, equally spaced from $\Delta E^{(1)} = 0.55$ Ryd to $\Delta E^{(5)} = (E_0 + I(^6D))/2$. The first value is approximately mid-way between the $Cr^+$ ($3d^5$) $^6S$ and $Cr^+$ ($3d^44s$) $^6D$ thresholds, and the last value is the maximum $\Delta E$ needed for the integration over $\Delta E$ when finding the total cross sections. A complete range of ejected-electron energies, $E_2$, was considered for each $\Delta E^{(k)}$, $k = 1, \ldots, 5$. Then, for each $E_2$, the cross sections for the physically correct value of $\Delta E$ were obtained by interpolating the results at the key values $\{\Delta E^{(k)}\}$.

Calculations have been performed for $E_0$ from 100 eV down to 10 eV. However, since the ionization potentials for $Cr^+$ ($3d^5$) $^6S$ and $Cr^+$ ($3d^44s$) $^6D$ are 6.765 eV and 8.287 eV, respectively, significant errors may arise from using a distorted-wave description of the ionizing electron at the lower values of $E_0$.

The most basic quantities that we have calculated are the contributions from each final symmetry $\lambda$ to the single differential cross section for production of each ionic state: $dQ^\lambda(^6S)/dE$ and $dQ^\lambda(^6D)/dE$. Integration of $dQ^\lambda(^6S)/dE$ with respect to $\Delta E$ gives the $\lambda$ contribution to the total cross section $Q^\lambda(^6S)$. Summation over $\lambda$ gives $dQ(^6S)/dE$ and $Q(^6S)$. Similarly, $Q^\lambda(^6D)$, $dQ(^6D)/dE$ and $Q(^6D)$ are obtained from $dQ^\lambda(^6D)/dE$. Finally, the cross sections for production of either ionic state are denoted by '$\Sigma$'. Thus, $Q(\Sigma) = Q(^6S) + Q(^6D)$ etc.

## 3. Results and discussion

### *3.1. Total cross sections*

Table 1 gives the results of the $R$-matrix calculation, and these results are also shown as the points in figure 1. A smooth interpolating spline can be fitted to $Q(^6D)$. However, this is not possible for $Q(^6S)$ because the $E_0$ dependence of the shapes of the resonances in $dQ(^6S)/dE$ causes the contribution to $Q(^6S)$ from each resonance to be non-monotonic in $E_0$, which leads to fluctuations in $Q(^6S)$ as a function of $E_0$

(see also section 3.3 below). Rather than resolving these small fluctuations by further computation, we have produced a 'best-smooth-curve' fit to $Q(^6S)$ by approximating $Q(\Sigma)$ by a least-squares spline, with the approximation to $Q(^6S)$ then given by subtracting the interpolatory spline approximation to $Q(^6D)$. These smooth curves are shown in figure 1. The broad features of the total cross sections are that $Q(\Sigma)$ has a maximum value of $30.3\,a_0^2$ at $E_0 = 31$ eV, and that the major contribution to $Q(\Sigma)$ comes from $Q(^6D)$ for energies above the maximum but from $Q(^6S)$ for energies below the maximum.

**Table 1.** Total cross sections for electron impact ionization of $Cr(3d^5 4s)\,^7S$, calculated by the $R$-matrix method of Bartschat and Burke (1987). $Q(^6S)$ and $Q(^6D)$ are the cross sections for production of $Cr^+(3d^5)\,^6S$ and $Cr^+(3d^4 4s)\,^6D$, respectively, and $Q(\Sigma) = Q(^6S) + Q(^6D)$. $E_0$ is the impact energy.

| $E_0$ (eV) | $Q(\Sigma)$ $(a_0^2)$ | $Q(^6S)$ $(a_0^2)$ | $Q(^6D)$ $(a_0^2)$ |
|---|---|---|---|
| 10.0 | 8.17 | 7.35 | 0.82 |
| 15.0 | 17.42 | 12.97 | 4.45 |
| 20.0 | 23.49 | 15.05 | 8.44 |
| 25.0 | 27.38 | 15.06 | 12.32 |
| 30.0 | 30.29 | 15.21 | 15.08 |
| 35.0 | 29.34 | 13.29 | 16.05 |
| 40.0 | 27.22 | 11.53 | 15.69 |
| 50.0 | 23.31 | 9.54 | 13.77 |
| 60.0 | 20.54 | 8.32 | 12.22 |
| 80.0 | 16.87 | 6.51 | 10.36 |
| 100.0 | 14.67 | 5.35 | 9.32 |

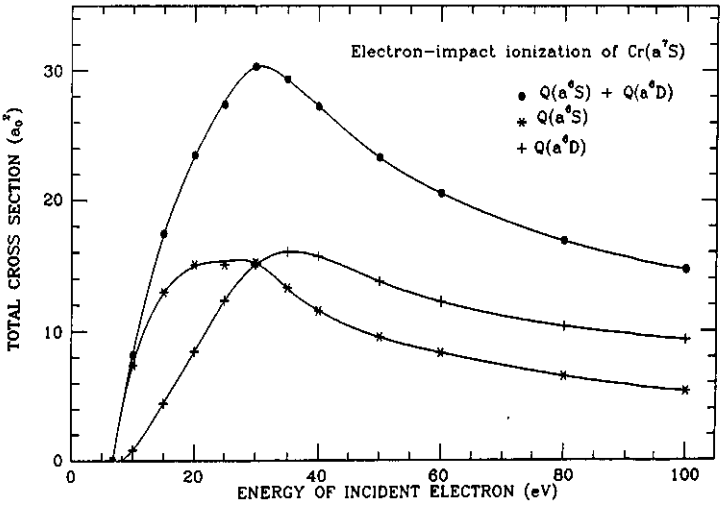


**Figure 1.** Total cross sections for electron impact ionization of $Cr(3d^5 4s)\,^7S$, producing $Cr^+(3d^5)\,^6S$ (*) or $Cr^+(3d^4 4s)\,^6D$ (+) or both (•), plotted against impact energy. The points are $R$-matrix results, the smooth curves are spline fits.

### *3.2. Convergence with respect to $\lambda$*

Figure 2 shows the relative sizes of $Q^\lambda(^6D)$ and $Q^\lambda(^6S)$. (In the $^6S$ case, it is only the contributions to $Q^\lambda(^6S)$ from above the $^6D$ threshold that are shown. However, as can be seen from figure 5 below, the relative sizes of the contributions to $Q^\lambda(^6S)$ from below the $^6D$ threshold are similar to those shown in figure 2.) For $Q^\lambda(^6D)$, the fall-off with increasing $\lambda$ is very satisfactory. For $Q^\lambda(^6S)$, the picture is less clear because both $Q^0(^6S)$ and $Q^1(^6S)$ are smaller than $Q^2(^6S)$, with $Q^0(^6S)$ particularly small. However, concentrating on $\lambda \geqslant 2$, we again conclude that truncation at $\lambda = 4$ is justified. For both $Q^\lambda(^6D)$ and $Q^\lambda(^6S)$ the fall-off with respect to $\lambda$ is approximately geometric, and hence we are able to estimate that the terms with $\lambda \geqslant 5$ would increase the cross sections by no more than 5%.

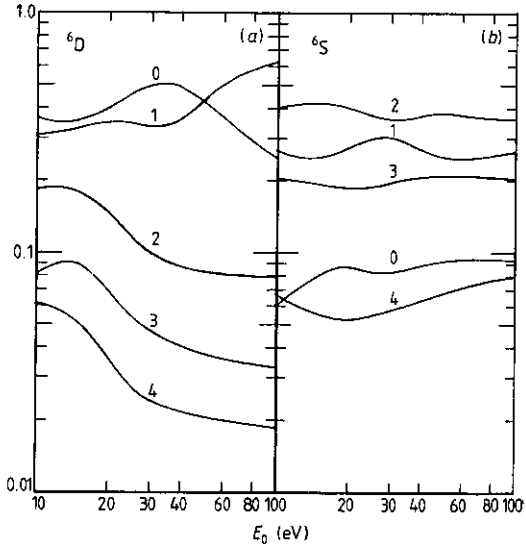


**Figure 2.** Relative contributions from various symmetries ($\lambda = 0, \ldots, 4$) to the total cross sections for production of (*a*) $Cr^+$ ($3d^4 4s$) $^6D$ and (*b*) $Cr^+$ ($3d^5$) $^6S$, plotted against impact energy.

### *3.3. Resonances in single differential cross section below the $^6D$ threshold*

Figure 3 shows $dQ(^6S)/dE$ plotted against energy loss $\Delta E$, for $\Delta E$ below the threshold for production of $Cr^+$ ($3d^4 4s$) $^6D$, for $E_0 = 20$ eV and $E_0 = 100$ eV. There are several series of resonances, due to the presence of quasibound states of Cr I of the form $3d^4 4s(^6D)\, nl\, ^7L$ ($L = 0, \ldots, 4$) lying in the $3d^5(^6S)\, kl_2\, ^7L$ continua. Although the positions of the resonances do not vary with $E_0$, the precise details of the shapes do, as is illustrated in figure 4 which shows $dQ(^6S)/dE$ in the neighbourhood of the resonance at 0.502 82 Ryd, for $E_0 = 20$ eV, $E_0 = 25$ eV and $E_0 = 30$ eV. Whereas the non-resonant background cross section is increasing steadily as $E_0$ decreases, the cross section at the resonance is least for $E_0 = 20$ eV. Hence, as $E_0$ decreases from 25 eV to 20 eV, $Q(^6S)$ departs from the behaviour predicted by

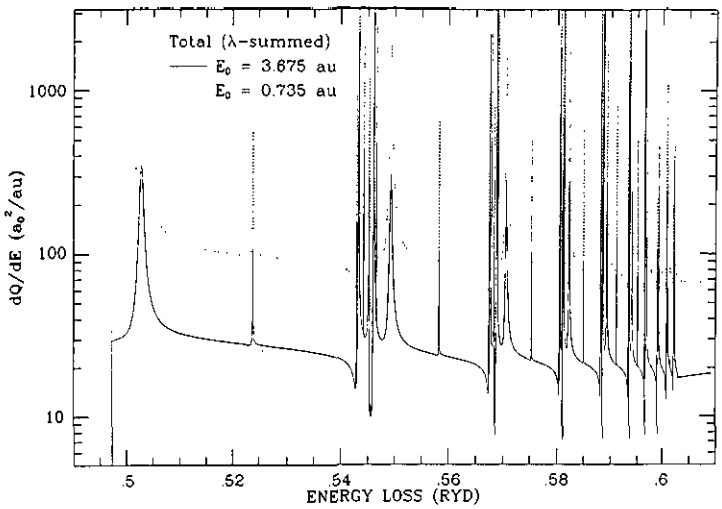


**Figure 3.** Single differential cross section plotted against energy loss, below the $Cr^+$ ($3d^4 4s$) $^6D$ threshold, for impact energies 20 eV (·····) and 100 eV (——).

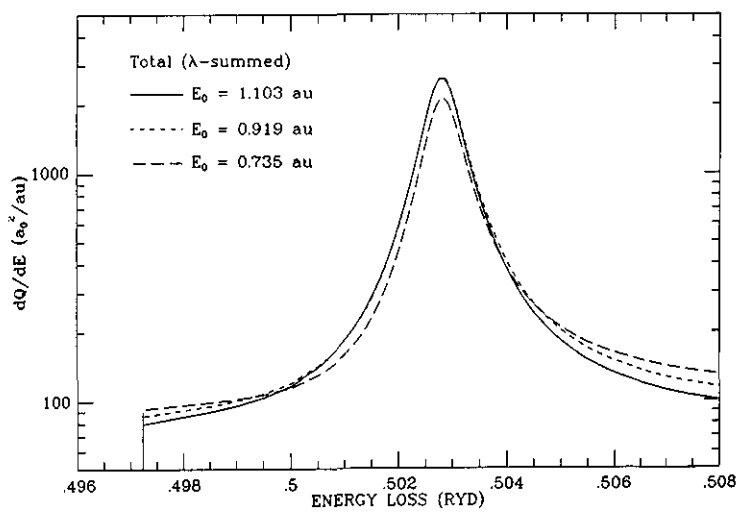


**Figure 4.** Single differential cross section plotted against energy loss in the neighbourhood of a resonance, for impact energies 20 eV (— — —), 25 eV (– – –) and 30 eV (——).

the non-resonant background alone. This explains the fluctuations in $Q(^6S)$ referred to above.

Regarding the contributions from various $\lambda$, figure 5 shows $dQ^{\lambda}(^6S)/dE$ below the $^6D$ threshold for $E_0 = 100$ eV. The independent variable in figure 5 is the effective quantum number $\nu$, where $\nu \equiv [1\,\mathrm{Ryd}/(I(^6D) - \Delta E)]^{1/2}$. Only a limited range of $\nu$ is shown, to illustrate the shapes of the resonances in each of the ten series. The pattern is similar for higher $\nu$. The strength and breadth of the $^7S$ resonances are noteworthy, and indicate strong coupling between the bound $3d^4(^5D)\,3d4s\,^7S$ state,

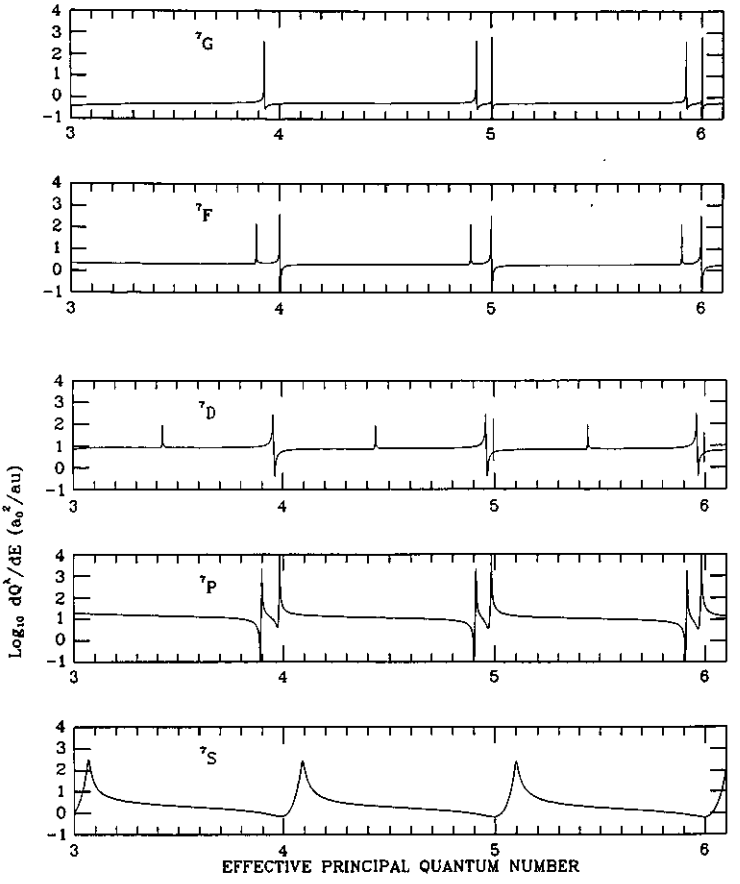


**Figure 5.** Contributions from each symmetry ($\lambda$) to the single differential cross section for energy losses below the $Cr^+$ ($3d^4 4s$) $^6$D threshold, for impact energy 100 eV. The energy loss is represented by its distance below this threshold via the effective quantum number.

the quasi-bound $3d^4(^5D)\,4snd\,^7S$ states and the continuum $3d^4(^5D)\,3dks\,^7S$ states.

Table 2 gives the details of the resonances for $\nu \leqslant 9$. The positions and widths were determined by fitting a Fano profile plus a linear background to each resonance (cf Stafford 1991). Rather than show $\Gamma$, the width in the energy $\Delta E$, the table shows $w \equiv \Gamma\nu^3/(2\,\mathrm{Ryd})$. The quantity $w$ is the width in the variable $\nu$, and demonstrates the uniformity within each series. The reliability of the calculated widths is reduced if the resonances are not well isolated (as in the $np\,^7P^o$ and $nf\,^7P^o$ series), or are excessively narrow (as in the $ng\,^7D$ and $ng\,^7G$ series). The assignment of principal quantum numbers to the s, p and d orbitals in table 2 is based on the designation given by Bashkin and Stoner (1981) for the observed bound levels that lie below the ionization limit. Also, the grouping of the terms arising from the same configuration is taken into account. Thus, for the $3d^4(^5D)\,4snd$ configurations, the fact that there are bound 4s4d $^7$D, $^7$F, $^7$G terms—but no 4s4d $^7$S—lying just below the ionization limit leads us to identify the lowest $^7$S resonance as 4d, and the next group as 4s5d $^7$S, $^7$D, $^7$G. For the $np\,^7P^o$, $^7F^o$ series, the designation of the bound $y\,^7P^o$ and $z\,^7F^o$ terms as 4p leads to the designation 6p for the lowest

**Table 2.** Rydberg resonances in $e + Cr^+$ scattering. The energy scale is $\Delta E$, the energy loss by the incident electron in the ionization of $Cr\,(3d^5 4s)\,{}^7S$. On this scale, the energies of $Cr^+\,(3d^5)\,{}^6S$ and $Cr^+\,(3d^4 4s)\,{}^6D$ are 0.497 2342 and 0.609 1208, respectively. All the resonances have classification $(3d^4 4s\,nl)\,{}^7L^\pi$. The table shows $nl$ beneath the symmetry ${}^7L^\pi$. The effective quantum number, $\nu$, refers to the energy of binding to the $Cr^+\,(3d^4 4s)\,{}^6D$ core. The scaled $\nu$ width, $\tilde{w}$, is the energy width in atomic units times $\nu^3 \times 10^4$.

| | | | Classification | | | | |
|---|---|---|---|---|---|---|---|
| $\Delta E$ (Ryd) | $\nu$ | $\tilde{w}$ | ${}^7S^e$ | ${}^7P^o$ | ${}^7D^e$ | ${}^7F^o$ | ${}^7G^e$ |
| 0.502 7962 | 3.067 | 120 | 4d | | | | |
| 0.523 9808 | 3.427 | 16 | | | 6s | | |
| 0.542 9796 | 3.888 | 5.1 | | | | 6p | |
| 0.543 3090 | 3.898 | 12 | | 6p | | | |
| 0.544 2749 | 3.927 | 3 | | | | | 5d |
| 0.545 2901 | 3.958 | 24 | | | 5d | | |
| 0.546 1383 | 3.985 | 5 | | 4f | | | |
| 0.546 6411 | 4.001 | 4 | | | | 4f | |
| 0.549 3461 | 4.091 | 133 | 5d | | | | |
| 0.558 3376 | 4.438 | 15 | | | 7s | | |
| 0.567 4652 | 4.900 | 4.9 | | | | 7p | |
| 0.567 6276 | 4.909 | 10 | | 7p | | | |
| 0.567 9355 | 4.928 | 2 | | | | | 6d |
| 0.568 4454 | 4.958 | 22 | | | 6d | | |
| 0.568 8457 | 4.983 | 8 | | 5f | | | |
| 0.569 0434 | 4.995 | — | | | 5g | | |
| 0.569 0984 | 4.999 | 5 | | | | 5f | |
| 0.569 1613 | 5.003 | 0.3 | | | | | 5g |
| 0.570 6714 | 5.100 | 137 | 6d | | | | |
| 0.575 3600 | 5.442 | 14 | | | 8s | | |
| 0.580 4457 | 5.905 | 4.9 | | | | 8p | |
| 0.580 5375 | 5.915 | 9 | | 8p | | | |
| 0.580 6645 | 5.928 | 2 | | | | | 7d |
| 0.580 9561 | 5.958 | 22 | | | 7d | | |
| 0.581 1753 | 5.982 | 9 | | 6f | | | |
| 0.581 2972 | 5.995 | — | | | 6g | | |
| 0.581 3193 | 5.997 | 6 | | | | 6f | |
| 0.581 3654 | 6.002 | 0.5 | | | | | 6g |
| 0.582 2885 | 6.105 | 139 | 7d | | | | |
| 0.585 0477 | 6.445 | 14 | | | 9s | | |
| 0.588 1695 | 6.909 | 4.8 | | | | 9p | |
| 0.588 2265 | 6.918 | 8 | | 9p | | | |
| 0.588 2888 | 6.928 | 1 | | | | | 8d |
| 0.588 4711 | 6.959 | 22 | | | 8d | | |
| 0.588 6036 | 6.981 | 10 | | 7f | | | |
| 0.588 6834 | 6.995 | — | | | 7g | | |
| 0.588 6938 | 6.997 | 6 | | | | 7f | |
| 0.588 7263 | 7.002 | 0.6 | | | | | 7g |
| 0.589 3275 | 7.108 | 139 | 8d | | | | |
| 0.591 0885 | 7.447 | 11 | | | 10s | | |
| 0.593 1417 | 7.911 | 4.2 | | | | 10p | |
| 0.593 1797 | 7.920 | 8 | | 10p | | | |
| 0.593 2135 | 7.929 | 2 | | | | | 9d |
| 0.593 3344 | 7.959 | 20 | | | 9d | | |
| 0.593 4216 | 7.981 | 10 | | 8f | | | |

**Table 2.** (continued)

| | | | Classification | | | | |
|---|---|---|---|---|---|---|---|
| $\Delta E$ (Ryd) | $\nu$ | $\tilde{w}$ | $^7S^e$ | $^7P^o$ | $^7D^e$ | $^7F^o$ | $^7G^e$ |
| 0.593 4760 | 7.995 | — | | | 8g | | |
| 0.593 4811 | 7.996 | 7 | | | | 8f | |
| 0.593 5047 | 8.002 | 0.8 | | | | | 8g |
| 0.593 9149 | 8.110 | 148 | 9d | | | | |
| 0.595 1091 | 8.448 | 16 | | | 11s | | |
| 0.596 5307 | 8.913 | 5.5 | | | | 11p | |
| 0.596 5569 | 8.922 | 7 | | 11p | | | |
| 0.596 5776 | 8.929 | 1 | | | | | 10d |
| 0.596 6629 | 8.959 | 21 | | | 10d | | |
| 0.596 7222 | 8.981 | 13 | | 9f | | | |
| 0.596 7612 | 8.995 | — | | | 9g | | |
| 0.596 7641 | 8.996 | 6 | | | | 9f | |
| 0.596 7813 | 9.002 | 0.6 | | | | | 9g |

resonance in table 2. Similarly, the designation of the bound f $^7$D term as 4s5s leads us to start the quasi-bound series at 6s. Finally, the assignment for the f and g orbitals is unambiguous because the large radii of these orbitals means that they have small quantum defects. This also explains the narrowness of these resonances. For the same reason, resonances involving h or i orbitals would not be expected to be significant, and indeed none were found. The $ng\,^7$G series has negative quantum defects, showing a repulsion by the core electrons. Similar observations have been made, in the context of photoionization, by Fernley *et al* (1987).

### *3.4. Single differential cross sections above the $^6$D threshold*

Figure 6 shows $dQ(^6S)/dE$ and $dQ(^6D)/dE$ plotted against $\Delta E$, for $\Delta E$ from the $^6$D threshold to the upper limit used in the integration over $\Delta E$, namely, $(E_0 + I(^6S))/2$ or $(E_0 + I(^6D))/2$. The graphs for the various $E_0$ can be distinguished by the fact that a higher incident energy corresponds to a larger upper limit. Note that, particularly for $dQ(^6S)/dE$ or for the higher $E_0$, the single differential cross sections are close to having a simple power-law dependence on $\Delta E$. That the $^6$D results change their form with decreasing $E_0$ more than is the case for $^6$S is probably related to the change with $E_0$ in the relative sizes of the $\lambda = 0$ and $\lambda = 1$ components of $dQ(^6D)/dE$ (cf figure 2).

## 4. Conclusions

We have calculated total and single differential cross sections for electron impact ionization of Cr ($3d^5 4s$) $^7$S, leading to production of $Cr^+$ ($3d^5$) $^6$S or $Cr^+$ ($3d^4 4s$) $^6$D, for a wide range of impact energies, from 10 eV (which is just above the $Cr^+$ ($3d^4 4s$) $^6$D threshold) to 100 eV, although the validity of a distorted wave method may be questioned at the lower energies. The total cross section has a maximum value of $30.3\,a_0^2$ at an impact energy of 31 eV. We have established that, for the total cross sections, it is sufficient to include the $2^\lambda$-pole components of the interaction with $\lambda \leqslant 4$. Below the $Cr^+$ ($3d^4 4s$) $^6$D threshold, the single differential cross section

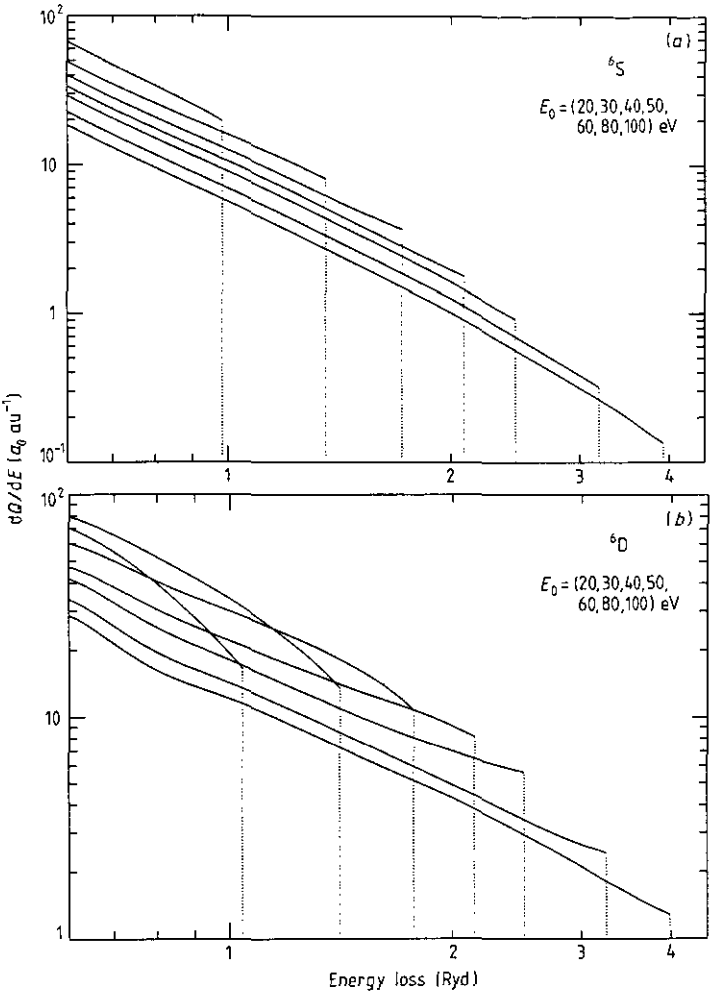


**Figure 6.** Single differential cross sections for production of (*a*) $Cr^+$ $(3d^5)$ $^6S$ and (*b*) $Cr^+$ $(3d^44s)$ $^6D$, plotted against energy loss, above the $Cr^+$ $(3d^44s)$ $^6D$ threshold, for impact energies 20, 30, 40, 50, 60, 80 and 100 eV. The cases can be distinguished by their upper limits.

for production of $Cr^+$ $(3d^5)$ $^6S$ exhibits pronounced resonances which contribute significantly to the total cross section. These resonances are due to autoionizing states that are incorporated automatically by the accurate treatment of the inner region in the *R*-matrix method. We have analysed the resonances in detail, identifying ten separate series.

## Acknowledgments

It is a pleasure to thank Dr R P Stafford for helpful discussions concerning analysis of resonances. This work was supported, in part, by JET under grant JT8/12784, by

NATO under grant CRG 900144, by the National Science Foundation under grant PHY-9014103 and by the Research Corporation under grant C-2640.

## References

Bartschat K 1992 *Comput. Phys. Commun.* to be submitted
Bartschat K and Burke P G 1987 *J. Phys. B: At. Mol. Phys.* **20** 3191
—— 1988 *J. Phys. B: At. Mol. Opt. Phys.* **21** 2969
Bartschat K, Reid R H G, Burke P G and Summers H P 1990 *J. Phys. B: At. Mol. Opt. Phys.* **23** L721
Bashkin S and Stoner J O 1981 *Atomic Energy-Levels and Grotrian Diagrams* vol III (Amsterdam: North-Holland)
Bures M, Jacquinot J, Stamp M, Summers H P, D'Ippolito D and Myra J 1990 *Plasma Phys. Control. Fusion* **31** 937
Clementi E and Roetti C 1974 *At. Data Nucl. Data Tables* **14** 177
Fernley J A, Taylor K T and Seaton M J 1987 *J. Phys. B: At. Mol. Phys.* **20** 6457
Jacubowicz H and Moores D L 1981 *J. Phys. B: At. Mol. Phys.* **14** 3733
Stafford R P 1991 *PhD Thesis* The Queen's University of Belfast